# Edge-Modification of Laponite with Dimethyl-octylmethoxysilane

**Lisa M. Daniel, Ray L. Frost • and Huai Yong Zhu**

*Inorganic Materials Research Program, School of Physical and Chemical Sciences, Queensland University of Technology, GPO Box 2434, Brisbane Queensland 4001, Australia.*

*Email: r.frost@qut.edu.au*

## Abstract

This study examines the edge modification of laponite, with a monoalkoxy silane, dimethyloctyl methoxysilane. The influence of ultrasonics, aging time and silane concentration on the resultant materials is examined. The silylated clays are characterized by XRD, IES, TGA, and Si-NMR. The amount of grafted silane was increased by increasing the ratio of silane to clay, sonication of the reaction mixture and ageing the reaction mixture for no more than 24 hours to avoid removal of grafted silane due to equilibrium effects.

*Key words:* laponite; silane, silylation, edge-modification, IES.

• Author to whom correspondence should be addressed (r.frost@qut.edu.au)

## 1. Introduction

Clays incorporated in polymeric materials, can alter properties of the polymer system, such as thermal and mechanical properties [1]. Studies of clay modification have been shown to have importnat surface properties [2-10] . The modification of clay surfaces from hydrophilic to hydrophobic to enhance their compatibility with polymeric materials has therefore attracted much attention [1, 11-13]. Clays have been organically modified by the ion exchange of the interlayer cations with large organic cations [14-18], and also by the reaction of the edge silanols with silanes [19-21].

Laponite, a synthetic hectorite, is one such clay employed for incorporation into plastic systems. It has a relatively small particle size, with a basic unit consisting of a layered hydrous magnesium silicate platelet of diameter 25-30 nm with a thickness of approximately 1 nm [22]. The unit cell consists of a sheet of six octahedrally co-ordinated $Mg^{2+}$ ions sandwiched between two layers of four tetrahedrally co-ordinated $Si^{4+}$ ions [23]. The cations are coordinated by 20 oxide ions and four hydroxyl groups [24]. Isomorphic substitution of the $Mg^{2+}$ ions with $Li^{+}$ ions, leads to the formation of a negative charge on the clay layer. This charge is balanced by the presence of sodium ions between the layers. The cation exchange capacity of laponite is 0.55mequiv per gram.

Laponite has reactive hydroxyl groups present on the edges in the form of SiOH groups, and within the interior of the clay sheet in the form of Mg-OH or Li-OH groups. In organic solvents, laponite exists in the form of tactoids with two or three clay sheets held together by long-range attractive forces [25]. Negative charges are

present in laponite in from both the isomorphic substitutions and the SiOH groups on the broken edges. The edge charges are pH dependent, with MgOH groups positive below a pH of 9, and SiOH groups negatively charged. The edge charge of laponite covers less than 10% of the overall CEC of the clay [25].

The formation of a siloxane linkage proceeds in two steps, hydrolysis and polymerization, as described by the following reactions.

$\equiv$Si-OEt + $H_2O$ → $\equiv$Si-OH + EtOH

$\equiv$Si-OH + OH-Si$\equiv$ → $\equiv$Si-O-Si$\equiv$ + $H_2O$

Silylation of laponite in organic media, such as toluene, allows for the formation of Si-O-Si linkages between the Si-OH bonds on the edge of laponite clay platelets, shown in Figure 1.

Covalently-functionalised Laponite clay particles have been synthesised through a condensation reaction of the clays edge silanol groups with mono- and tri-alkoxy silanes [26, 27]. Trialkoxy silanes were found to link the clay sheets together, increasing the clay basal spacing and surface area and making them nondispersible in water. Monoalkoxy silanes however form a flat monolayer on the edge of the clay plates [25], and have a minimal effect on the basal spacing and surface area of the clay. Redispersion of clays modified with monoalkoxy silanes, is easier due to the smaller resultant particle size.

The aim of this paper is to describe the silylation of laponite with the monoalkoxysilane, dimethyl-octylmethoxysilane, and to examine the effect of synthesis conditions on the resultant properties of the material using infrared emission

absorption, $^{29}$Si-NMR, thermogravimetric analysis, BET $N_2$ sorption and x-ray diffraction.

## 2. Experimental

### 2.1 Materials

Laponite clay (Laponite RD) was obtained from Fernz Specialty Chemicals, Australia and used as received. The clay powder has the chemical formula, $Na_{0.67}K_{0.01}(Si_{7.95}Al_{0.05})$-$(Mg_{5.48}Li_{0.38}Ti_{0.01})O_{20}(OH)_4$, a BET specific surface area of 336.7$m^2$/g and a cation exchange capacity of 0.75 meq/g of clay. Dimethyl-octylmethoxysilane, (MW = 202.41 ) obtained from Sigma Aldrich, was used without purification. Toluene AR grade was purchased from Sigma-Aldrich and used as recieved, without further purification.

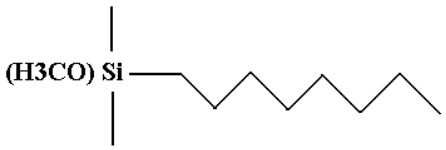


Structure: Dimethyl octylmethoxysilane ($C_9H_{26}OSi$)

### 2.2. Silylation of Laponite with Dimethyl-octylmethoxysilane

To a dispersion of laponite in toluene (10g $L^{-1}$), dimethyl-octylmethoxysilane of concentrations of (1, 5, 10 and 20 mmol/g laponite) were added, the mixture

sonicated for 20 minutes and then stirred for 72 hours at room temperature. The powder sample was recovered via centrifugation and then washed three times with toluene to remove excess silane. Further samples were prepared with silane to clay ratios of 5mmol/g both with and without sonication periods of 80 minutes. The aging time employed in these samples was examined by preparing samples aged for periods of 24, 48 and 72 hours. Sample were given names incorporating the synthesis parameters of ultrasonic time, aging time and silane concentration. The sample labelled Si-L20-72-1 for example, was prepared with 20 minutes of sonication, an aging time of 72 hours and a silane concentration of 1mmol silane per gram laponite.

## 2.3 Characterisation

### *2.3.1 Infrared Emission Spectroscopy*

FTIR emission spectroscopy was carried out on a Nicolet Fourier transform infrared spectrometer equipped with a MCT/A detector, which was modified by replacing the IR source with an emission cell. Approximately 0.2 mg of the powder sample was spread as a thin layer on a 6 mm diameter platinum surface and held in an inert atmosphere within a nitrogen-purged cell during heating. The infrared emission cell consists of a modified atomic absorption graphite rod furnace, which is driven by a thyristor-controlled AC power supply capable of delivering up to 150 A at 12 V. A platinum disk acts as a hot plate to heat the sample and is placed on the graphite rod. An insulated 125-μm type R thermocouple was embedded inside the platinum plate in such a way that the thermocouple junction was < 0.2 mm below the surface of the platinum. Temperature control of ± 2 ◦C at the operating temperature of the clay sample was achieved by using a Eurotherm Model 808 proportional temperature

controller, coupled to the thermocouple. The emission spectra were collected at intervals of 50 ◦C over the range 100–800 ◦C. The time between scans (while the temperature was raised to the next hold point) was ±100 s. The spectra were acquired by the co-addition of scans for each of the test temperatures over the range. To improve resolution at lower temperatures, 1024 scans were employed, and this number decreased as the temperature and corresponding amount of radiation emitted from the sample increased also.

Spectral manipulation including baseline adjustment, smoothing and normalisation were performed using the Spectracalc software package GRAMS (Galactic Industries Corporation, NH, USA). Band component analysis was undertaken using the Jandel 'Peakfit' software package which enabled the type of fitting function to be selected and allows specific parameters to be fixed or varied accordingly. Band fitting was done using a Lorentz-Gauss cross-product function with the minimum number of component bands used for the fitting process. The Gauss-Lorentz ratio was maintained at values greater than 0.7 and fitting was undertaken until reproducible results were obtained with $r^2$ values greater than 0.995.

*2.3.2. Si-NMR*

29Si NMRspectra were recorded on a double-channel Varian InfinityPlus 400 spectrometer, equipped with a 7.5 mm cross-polarization (CP)-MAS probehead, working at 79.44 MHz. $^{29}$Si-single pulse excitation spectra were recorded for samples Laponite, Si-L0-72 and Si-L80-72 with a recycle delay of 100 s.

*2.3.3. Thermogravimetric Analysis*

Thermal decomposition of the silylated clay was carried out in a TA® Instruments incorporated high-resolution thermogravimetric analyzer (series Q500) in a flowing nitrogen atmosphere (80 $cm^3$/min). Approximately 50mg of sample was heated in an open platinum crucible at a rate of 10.0 °C/min up to 1000°C. The following equation, adapted from work by Herrera et al. was used to determine the amount of grafted silane based on the weight loss between 200 and 550ºC, $W_{200\text{-}550}$ [28]. As pure laponite exhibits a mass loss in this region due to the removal of water, this figure is subtracted from the weight loss of the silylated samples, to give a more correct value of $W_{200\text{-}550}$ attributed to the silane loss.

$$\text{Grafted amount (mequiv/g)} = \frac{10^3 W_{200-550}}{(100 - W_{200-550})M} \quad (1)$$

where M (g/mol) is the molecular weight of the grafted silane molecules. To determine the grafting yield, corresponding to the percentage of silane molecules successfully grafted, the following equation was employed.

$$\text{Grafting yield (\%)} = \text{graft density x } 100/[\text{silane}] \quad (2)$$

where [silane] (mequiv/g) is the initial silane concentration.

*2.3.5. X-ray diffraction*

XRD analyses of pressed powder samples, were performed on a Philips PANalytical X'Pert PRO X-ray diffractometer (radius: 240.0 mm). Incident X-ray radiation was produced from a line focused PW3373/10 Cu X-ray tube, operating at 40 kV and 40 mA, providing a $K\alpha_1$ wavelength of 1.54 Å. The incident beam was monochromated through a 0.020 mm Ni filter then passed through a 0.04 rad. Soller

slit, a 15 mm fixed mask and a ½° fixed anti scatter slit. After interaction with the sample, the diffracted beam passed though a secondary 0.04 rad. Soller slit and a 0.25° progressive divergence slit before detection by an X'Celerator RTMS detector. The detector was set in scanning mode, with an active length of 2.022 mm. Samples were analysed utilising Bragg-Brentano geometry over a range of 1.5 – 70° 2θ with a step size of 0.02° 2 θ, with each step measured for 12.1 seconds.

## 3. Results and Discussion

### *3.1. $^{29}$Si-Nuclear Magnetic Resonance*

In $^{29}$Si NMR spectroscopy, peaks are assigned the letters, $Q_n$, $T_n$, $D_n$, $M_n$, based on the number of oxygen atoms bonded to the Si atom, 4, 3, 2 and 1 respectively, where and n is the number of oxygen atoms bonded to a further Si atom. In Figure 2, Laponite exhibits two main peaks at -96 ppm and -86 ppm attributed to Q3 and Q2 sites respectively [29]. The Q3 peaks arise from the *Si*$(OMg)(OSi)_3$ silicon nuclei within the tetrahedral sheets [15]. The Q2 peak is attributed to the presence of silanols, *Si*$(OMg)(OSi)_2(OH)$, both at the broken edges of the clay sheet and due to defects within the clay structure.

Silylation of the samples with a monoalkoxy silane leads to a reduction in the intensity of the Q2 peak and a corresponding increase in the Q3 peak, due to the addition of the silane molecule to the silanols on the edges of the clay sheets, observed in Figure 3. A small M1 peak at approximately 16 ppm is expected to occur, attributed to the Si atom of the silane grafted to the clay edge [23]. The Si NMR analysis of Si-L80-72-5 failed to cover this region, however in the sample Si-

L0-72-5, a very small peak is present at 17ppm. In addition to this, both silylated samples prepared in this research, do exhibit a reduction in the ratio of the Q2 to Q3 peak intensities, consistent with the successful silylation of the laponite plates.The Q2 signal, with a chemical shift of approximately -86.2ppm, in laponite, is found to split into three bands for the sample, Si-L80-72-5, with chemical shifts of approximately -85.6, -86.6 and -88.5 ppm. This suggests that the three signals arise from three different Q2 silicon species within the silylated sample. The Q2 peak in Si-L0-72-5 also exibits a slight negative shift. This indicates that a particular Q2 species is involved in the silylation reaction, as the signal shifts away from this site. It would therefore be assumed that the Q2 signal arising from the silanols on the edge of the clay is located at approximately -85.5 ppm. The lack of resolution of the laponite Q2 peak has been attributed to the higher structural disorder induced by the greater presence of water in the sample [15]. The increased resolution of the sonicated sample when compared to the unsonicated sample, is likely due to the forced exfoliation of the clay that occurs with sonication and the subsequent evacuation of water molecules from the interlayer spacing of the clay.

### *3.2. Infrared Emission Spectroscopy*

The infrared emission spectra of laponite is shown in Figure 4. At temperatures below and including 200ºC, the high wavelength region of the laponite spectrum is dominated by various stretching vibrations of the hydroxyl groups bonded to metallic cations and to water molecules. Upon heating, the hydroxyl peaks become more defined due to the removal of numerous water peaks that obstruct their view. The peak at approximately 3665 $cm^{-1}$, is attributed to the Mg-OH stretching vibration

of the magnesium ion present in the octahedral sheet of the clay [28]. The peak at 3730 $cm^{-1}$ corresponds to the Si-OH stretching of the silanol groups present on the edge of the clay. At approximatley 700 ºC, the water peaks are eliminated and these two hydroxyl peaks are all that remain in the region spanning from 3400-3800$cm^{-1}$. The relative intensity of the Si-OH peak to the Mg-OH peak remains constant throughout the analysis. At 800 ºC, these peaks disappear due to the dehydroxylation of the laponite.

Figure 5 shows the spectra of the a silylated laponite, at temperatures spanning from 200 to 550 ºC. In this figure, it can be observed that at temperatures below and incuding 200 ºC, the same peaks attributed to hydroxyls and water are present. However, further peaks are also present at 2927 and 2860 $cm^{-1}$ due to the presence of C-H stretching in the attached silane molecule. At temperatures below and including 300 ºC, the relative intensity of the Si-OH peak to the Mg-OH peak is the same. However, above at 400 ºC, the Si-OH peak increases in intensity compared to the Mg-OH peak, due to the reformation of the Si-OH bonds upon degradation of the attached silane molecule. At 550 ºC, the C-H stretching bands disappear, marking the complete removal of the silane from the clay. The inaccessibility of the Mg-OH sites within the clay structure, ensures that the silane selectively bonds with the exposed Si-OH regions [28].

### *3.3. Thermogravimetric Analysis*

Laponite exhibits a sharp mass loss up to 150 ºC, due to the removal of adsorbed water. A further small mass loss is observed over the region of 200-550 ºC, due to the removal of interlayer water. A final mass loss occurs in the temperature region spanning from 550-800 ºC due to the dehydroxylation of laponite.

In the thermograms of the silylated samples, the mass loss attributed to the removal of adsorbed water is reduced, whilst the loss in the 200-550 ºC region is increased due to the removal of grafted silane. Dehydroxylation again occurs in the region from 550-800 ºC. The thermograms of laponite and the silylated samples are displayed in Figure 6 and the thermogravimetric data contained in Table 2.

The maximum grafted amount achieved was for sample Si-L20-72-20, with 0.097meq/g. Herrera et al. have reported the grafting of a monoalkoxy silane, (γ-MPDES, $C_{10}H_{22}O_3Si$) to laponite, with a grafting amount of 0.35 mequiv/g [28]. It is possible this amount is so high because they did not take into account the interlayer water loss that occurs in the temperature range of 200 to 600ºC in their calculations, or the mass loss due to the commencement of dehydroxylation at 550 ºC.

From Figure 7, it can be seen that sonication slightly increases the grafted amount of silane. This is likely to be due to the forced exfoliation of the clay that can occur with sonication, which exposes more Si-OH regions for reaction with the silane. For both the sonicated and unsonicated samples, a similar trend in the effect of aging time on the grafted amount was observed. The grafted amount was greatest for

samples aged for 24 hours, then 48 hours and lastly 72 hours. This reduction in the grafted amount of silane with aging time, is in conflict with results published by Herrera et al, who found a maximum grafted amount of 0.5 mmol of monoalkoxysilane/g of clay was achieved quite quickly and remained relatively constant over a period of 3 weeks [28]. It could be assumed that the silane binds to the clay rather quickly, but with time, is removed from the clay by the reaction with other species within the system, such as water eliminated from the clay interlayer, or the methanol produced via the initial hydrolysis of the silane molecule.

For samples prepared with varying silane concentrations, a trend is observed, in which the greater the concentration of silane, the greater the grafted amount, shown in Figure 8. The CEC of laponite is 0.55mequiv per gram of clay and 10% of this is from the edges of the laponite plates. Therefore if complete, selective silylation of the edges of the clay plates were to occur, it could be expected that 0.055mequiv of silane would bind to the clay. The sample prepared with 1 mmol silane/g clay, almost double that expected to participate in the edge modification, was found to have a grafted amount of 0.02 mmol/g of clay. Over the 72 hour period, it fails to react to completion, due to the equilibrium that was identified earlier between the silylated sample and the methanol in the system. The sample prepared with 20mmol silane/g clay has a grafted amount of 0.087, greater than the edge CEC. It can be expected that by using such a high concentration of silane, the equilibrium effects are minimal and silylation occurs not only on the edges, but also at other Si-OH sites within the clay. The greater grafted amount could also possibly be due to a degree of adsorption of excess silane onto the clay surface.

*3.4. X-Ray Diffraction*

The X-ray diffraction pattern of laponite and the silylated laponites is shown in Figure 9. Pure laponite exhibits a somewhat broad XRD pattern due to low crystallinity and small particle size. It has a broad peak at approximately 5.6º 2θ, attributed to the 001 crystal plane or basal spacing of the clay. Further peaks are present at values of 19.4◦, 27.5 º, 33.7 º, and 60.4 º corresponding to (100), (005), (110), and (300) crystal planes, respectively [30]. The XRD patterns of the silylated samples exhibit the same set of peaks. There is no shift observed in the (001) peak, indicating there has been no silane intercalated within the clay layers as the basal spacing remains the same.

## 5. Conclusions

Dimethyloctyl methoxysilane has been successfully grafted onto the edges of laponite clay plates. The grafted amount was found to increase when the system is sonicated, due to the forced exfoliation of the clay and consequent exposure of more reactive Si-OH sites. Furthermore, increases in grafted amount were found when samples were not left to age for more than 24 hours. After this time, an equilibrium occurs in which the attached silane molecules cleave from the clay and react with either water in the system released from within the clay or methanol which is a result of the initial hydrolysis of the silane molecule. Another factor affecting grafted amount is the concentration of the silane in the reaction. Samples prepared with high silane concentrations are less affected by the equilibrium conditions that occur in the system, and the grafted amount achieved is higher than that expected for complete

edge silylation of the clay. This greater amount could be due to the adsorption of silane onto the clay surface, and/or the reaction of the silane with clay silanols less readily accessible than those on the edges of the clay plates.

## 6. Acknowledgments

The financial and infra-structure support of the Cooperative Research Centre for Polymers and the Queensland University of Technology, Inorganic Materials Research Program is gratefully acknowledged. The Australian Research Council (ARC) is thanked for funding the instrumentation.

## 7. References


[1] S.-S. Lee, J. Kim, Journal of Polymer Science, Part B: Polymer Physics 42 (2004) 2367-2372.
[2] L.M. Daniel, R.L. Frost, H.Y. Zhu, J. Colloid Interface Sci. 316 (2007) 72-79.
[3] W. Shen, H. He, J. Zhu, P. Yuan, R.L. Frost, J. Colloid Interface Sci. 313 (2007) 268-273.
[4] Y. Xi, R.L. Frost, H. He, J. Colloid Interface Sci. 305 (2007) 150-158.
[5] Y. Xi, Q. Zhou, R.L. Frost, H. He, J. Colloid Interface Sci. 311 (2007) 347-353.
[6] R.L. Frost, E. Mendelovici, J. Colloid Interface Sci. 294 (2006) 47-52.
[7] E. Horvath, J. Kristof, R.L. Frost, E. Jakab, E. Mako, V. Vagvoelgyi, J. Colloid Interface Sci. 289 (2005) 132-138.
[8] R.L. Frost, E. Horvath, E. Mako, J. Kristof, J. Colloid Interface Sci. 270 (2004) 337-346.
[9] R.L. Frost, E. Horvath, E. Mako, J. Kristof, T. Cseh, J. Colloid Interface Sci. 265 (2003) 386-395.
[10] R.L. Frost, J. Kristof, J.T. Kloprogge, E. Horvath, J. Colloid Interface Sci. 246 (2002) 164-174.
[11] J.H. Shim, J.H. Joo, S.H. Jung, J.-S. Yoon, Journal of Polymer Science, Part B: Polymer Physics 45 (2007) 607-615.
[12] R. Sudip, A.K. Bhowmick, Rubber Chemistry and Technology 65 (2003) 1091.
[13] Y. Zhang, D.I. Gittins, D. Skuse, T. Cosgrove, J.S. Van Duijneveldt, langmuir 23 (2007) 3424-3431.
[14] P.A. Wheeler, J. Wang, J. Baker, L.J. Mathias, Chemistry of Materials 17 (2005) 3012-3018.
[15] S. Borsacchi, M. Geppi, L. Ricci, G. Ruggeri, C.A. Veracini, Langmuir 23 (2007) 3953-3960.
[16] J. Connolly, J.S. van Duijneveldt, S. Klein, C. Pizzey, R.M. Richardson, Langmuir 22 (2006) 6531-6538.
[17] E.S.H. Leach, A. Hopkinson, K. Franklin, J.S. Van Duijneveldt, Langmuir 21 (2005) 3821-3830.
[18] H.Y. Zhu, Z. Ding, C.Q. Lu, G.Q. Lu, Applied Clay Science 20 (2002) 165-175.
[19] H. He, J. Duchet, J. Galy, J.-F. Gerard, Journal of Colloid and Interface Science 288 (2005) 171-176.
[20] A.M. Shanmugharaj, Y. Rhee Kyong, H. Ryu Sung, J Colloid Interface Sci FIELD Full Journal Title:Journal of colloid and interface science 298 (2006) 854-859.
[21] J. Zhang, R.K. Gupta, C.A. Wilkie, Polymer 47 (2006) 4537-4543.
[22] H.J.M. Hanley, C.D. Muzny, B.D. Butler, Langmuir 13 (1997) 5276-5282.
[23] N.N. Herrera, J.-M. Letoffe, J.-L. Putaux, L. David, E. Bourgeat-Lami, Langmuir 20 (2004) 1564-1571.
[24] L.A.S.d.A. Prado, C.S. Karthikeyan, K. Schulte, S.P. Nunes, I.L. de Torriani, Journal of Non-Crystalline Solids 351 (2005) 970-975.
[25] E. Bourgeat-Lami, N.N. Herrera, J.-L. Putaux, S. Reculusa, A. Perro, S. Ravaine, C. Mingotaud, E. Duguet, Macromolecular Symposia 229 (2005) 32-46.
[26] N.N. Herrera, J.-M. Letoffe, J.-L. Putaux, L. David, E. Bourgeat-Lami, Langmuir 20 (2004) 1564-1571.
[27] P.A. Wheeler, J. Wang, J. Baker, L.J. Mathias, Chemistry of Materials 17 (2005) 3012-3018.
[28] N.N. Herrera, J.-M. Letoffe, J.-P. Reymond, E. Bourgeat-Lami, Journal of Materials Chemistry 15 (2005) 863-871.
[29] L. Delevoye, J.L. Robert, J. Grandjean, Clay Minerals 38 (2003) 63-69.
[30] P.X.P. Highscore.

| Samples | $Q_3$ Chemical Shift (ppm) | $Q_2$ Chemical Shifts (ppm) | | | $M_1$ Chemical Shift (ppm) | $Q_2/Q_3$ Peak Intensity % |
|---|---|---|---|---|---|---|
| Laponite | -96.2 | | -86.2 | | | 11.28 |
| Si-L0-72 | -96.2 | | -86.6 | | 17.0 | 10.31 |
| Si-L80-72 | -96.2 | -85.6 | -86.6 | -88.5 | | 10.55 |

**Table 1 $^{29}$Si-NMR Relative Peak Intensities**

| | Weight Loss (%)[a] | Corrected Weight Loss (%)[b] | Grafted Amount (mequiv/g)[c] | Grafted Yield (%)[d] | % of Edge CEC |
|---|---|---|---|---|---|
| **Laponite** | 2.58 | 0 | - | - | - |
| **Si-L0-72** | 3.13 | 0.55 | 0.027 | 0.55 | 49.7 |
| **Si-L80-72** | 3.43 | 0.85 | 0.042 | 0.85 | 77.0 |
| **Si-L80-48** | 3.65 | 1.07 | 0.053 | 1.07 | 97.2 |
| **Si-L0-48** | 3.65 | 1.07 | 0.053 | 1.07 | 97.2 |
| **Si-L0-24** | 3.8 | 1.22 | 0.06 | 1.22 | 110.94 |
| **Si-L80-24** | 3.260 | 1.130 | 0.056 | 1.129 | 102.66 |
| **Si-L20-72-1** | 2.9 | 0.32 | 0.02 | 1.59 | 28.84 |
| **Si-L20-72-5** | 3.27 | 0.69 | 0.03 | 0.69 | 62.41 |
| **Si-L20-72-10** | 3.37 | 0.79 | 0.04 | 0.39 | 71.53 |
| **Si-L20-72-20** | 3.870 | 1.740 | 0.087 | 0.437 | 159.06 |

[a] Weight loss between 200 and 550ºC. [b] Weight loss minus water loss [c]Determined using equation 1. [d] Determined using equation 2.

**Table 2 Thermogravimetric data of laponite and silylated laponites**

*List of Figures*

*List of Tables*

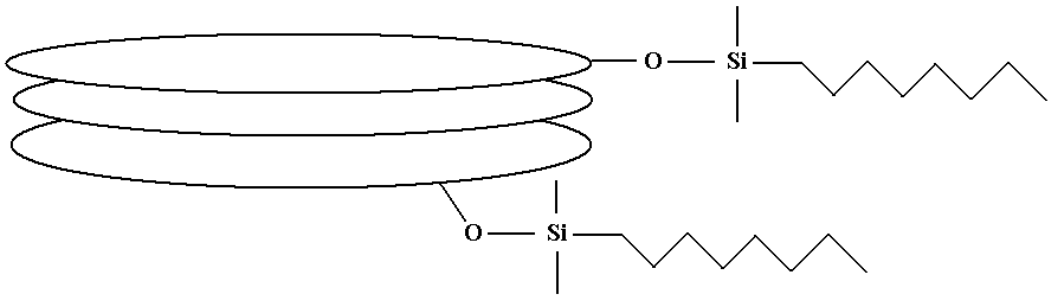


**Figure 1**

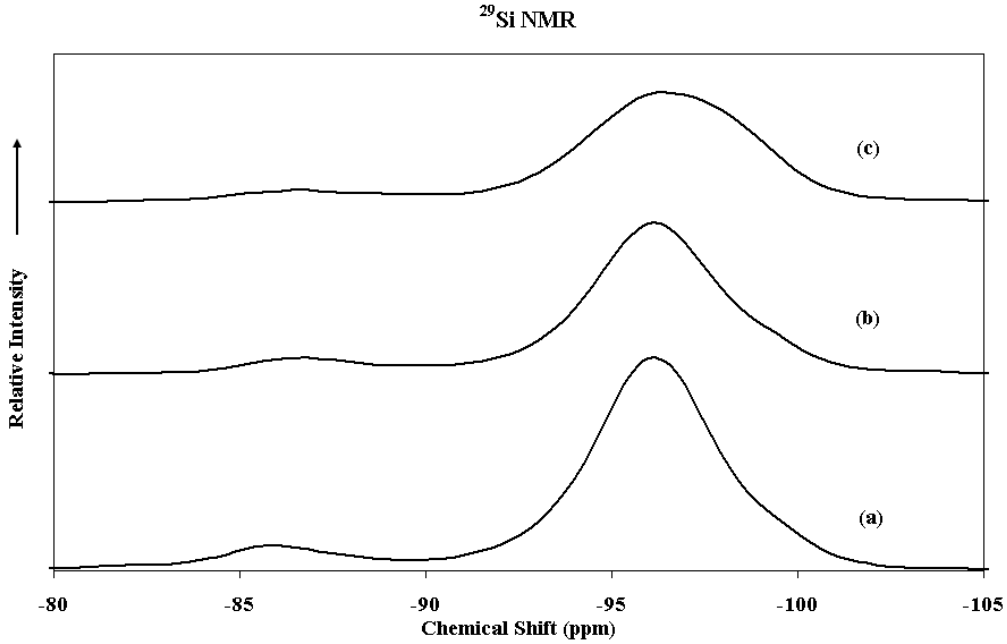
$^{29}$Si NMR
Relative Intensity
(c)
(b)
(a)
-80
-85
-90
-95
-100
-105
Chemical Shift (ppm)

**Figure 2**

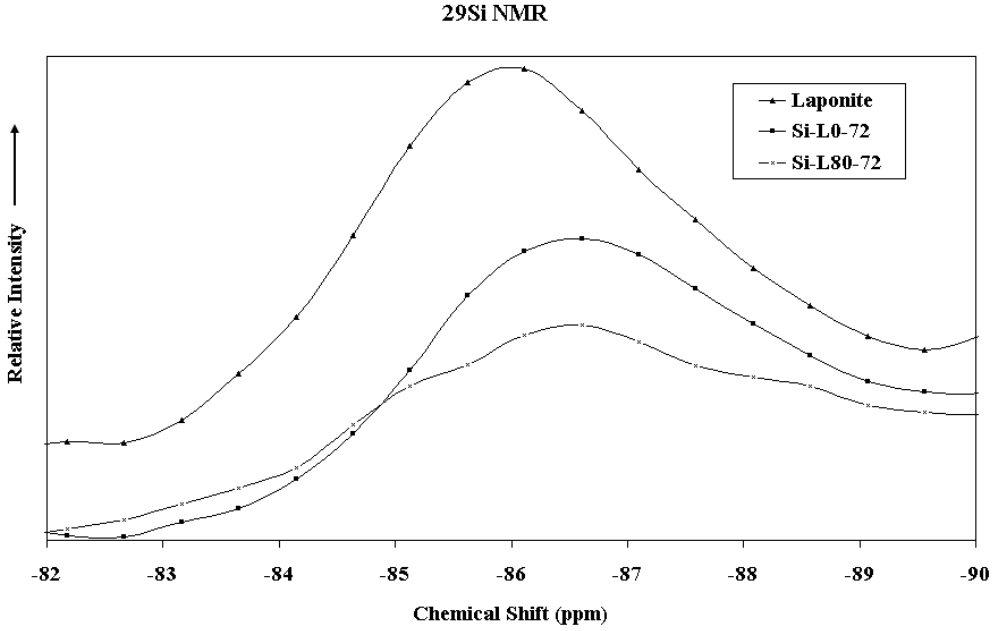
29Si NMR
Laponite
Si-L0-72
Si-L80-72
Relative Intensity
-82
-83
-84
-85
-86
-87
-88
-89
-90
Chemical Shift (ppm)

**Figure 3**

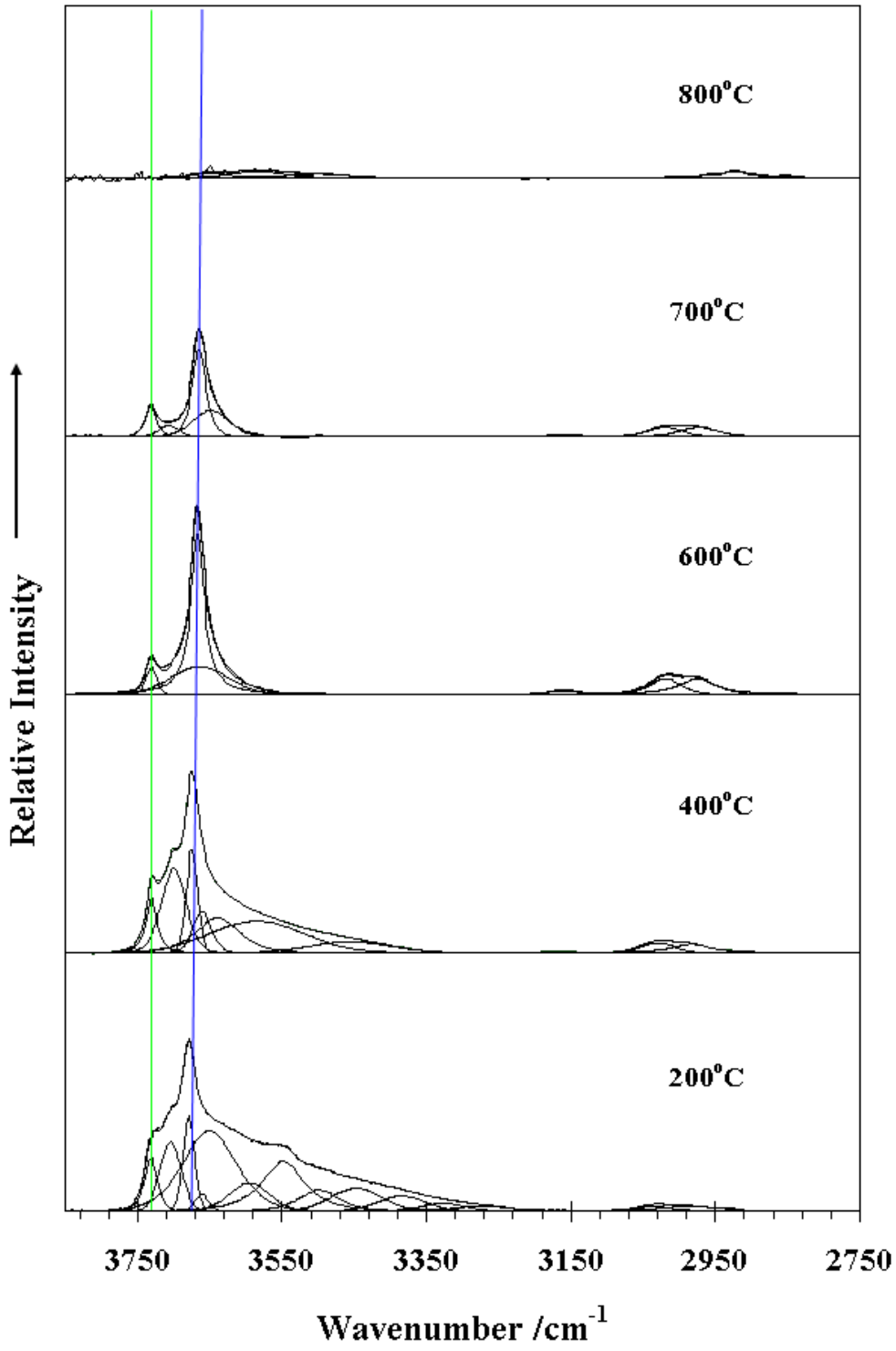
800°C
700°C
600°C
400°C
200°C
Relative Intensity
3750
3550
3350
3150
2950
2750
Wavenumber /cm-1

**Figure 4**

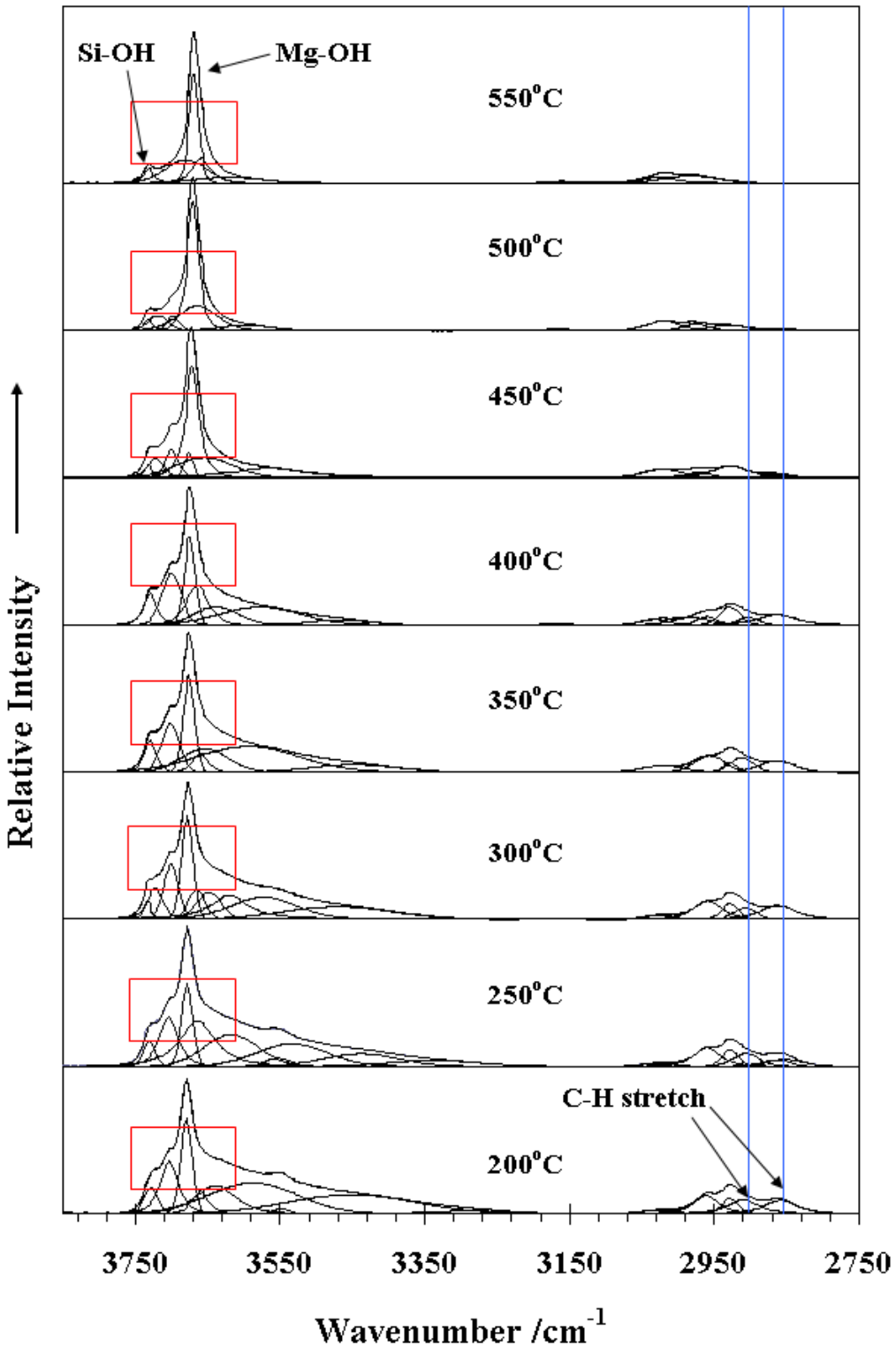
Si-OH
Mg-OH
550°C
500°C
450°C
400°C
350°C
300°C
250°C
C-H stretch
200°C
Relative Intensity
3750
3550
3350
3150
2950
2750
Wavenumber /cm-1

**Figure 5**

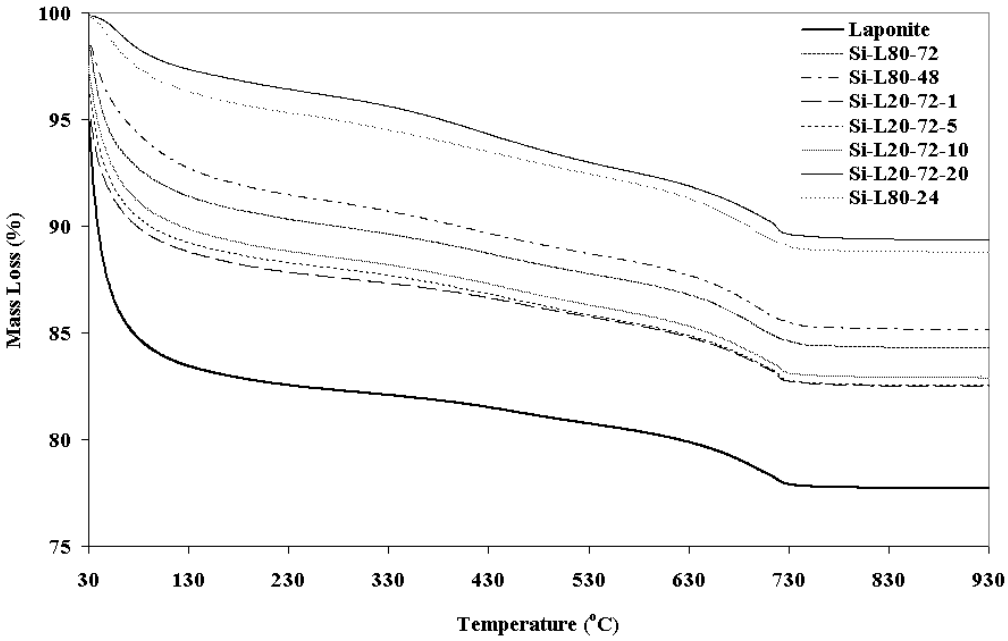
Laponite
Si-L80-72
Si-L80-48
Si-L20-72-1
Si-L20-72-5
Si-L20-72-10
Si-L20-72-20
Si-L80-24
Mass Loss (%)
100
95
90
85
80
75
30
130
230
330
430
530
630
730
830
930
Temperature (°C)

**Figure 6**

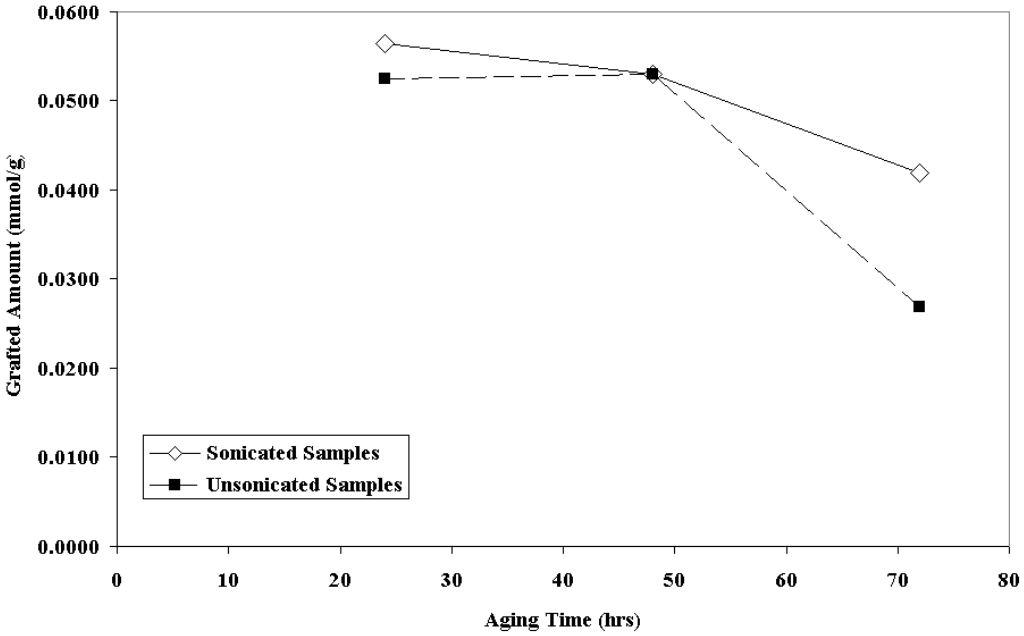
0.0600
0.0500
0.0400
0.0300
0.0200
0.0100
0.0000
Grafted Amount (mmol/g)
0
10
20
30
40
50
60
70
80
Aging Time (hrs)
Sonicated Samples
Unsonicated Samples

**Figure 7**

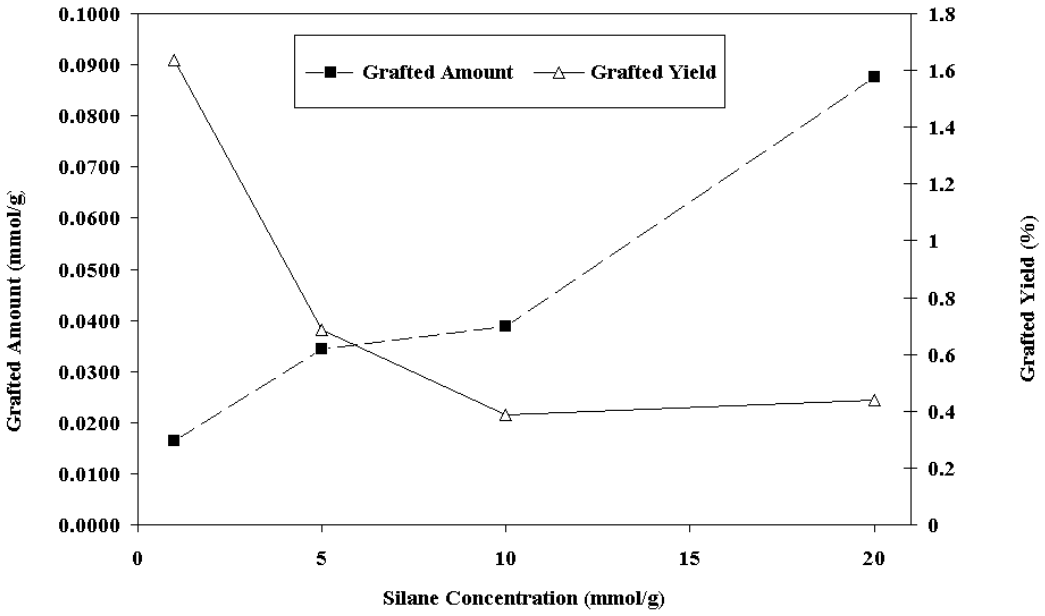
Grafted Amount
Grafted Yield
Grafted Amount (mmol/g)
Grafted Yield (%)
Silane Concentration (mmol/g)
0.1000
0.0900
0.0800
0.0700
0.0600
0.0500
0.0400
0.0300
0.0200
0.0100
0.0000
1.8
1.6
1.4
1.2
1
0.8
0.6
0.4
0.2
0
0
5
10
15
20

**Figure 8**

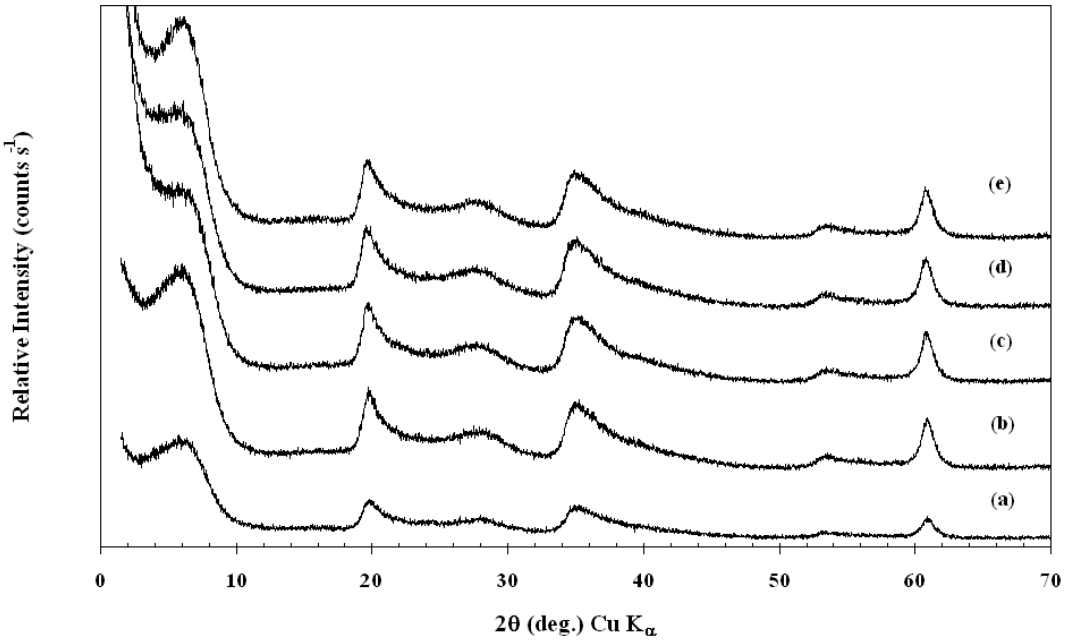
Relative Intensity (counts s-1)
(e)
(d)
(c)
(b)
(a)
0
10
20
30
40
50
60
70
2θ (deg.) Cu Kα

**Figure 9**